In this study, authors investigate chemical composition of particulate matter in Beijing, China and contrast these results with the measured aerosol optical parameters. The results of the manuscripts shed new light on how chemical composition influences the optical properties of the aerosol particles and introduces a new method for analyzing the collected particulate matter. The paper is overall well written and in scope of Atmospheric Chemistry and Physics journal but needs some corrections before publication.

Reply: We are very grateful for the positive comments and helpful suggestions. We have carefully revised our manuscript accordingly.

Major comments:

Section 2.2 (Offline FIGAERO-CIMS analysis): Major part of this section is left out to be detailed in future publication. Even though I understand the reasoning behind the decision, I feel that too many details are missing. In this state I feel that I cannot assess the credibility of the method and hence the results shown in the paper. The authors should present the draft of this future publication showing the main details of the methodology, or the used methodology should be presented in more detail in the current manuscript or in its supplement.

Reply: We realize that how we formulated this part of the method descriptions in the submitted manuscript may have been slightly misleading. The FIGAERO-CIMS has been used in offline mode previously (Huang et al., 2019a; Siegel et al., 2021), and the future publication mentioned merely provides an in-depth characterization and recommendations for best practices of this method. Here we largely followed the methodology used in those previous studies but needed to make adjustments to reduce reagent ion depletion due to high filter mass loadings. This is now explained in the SI as following, together with more information on how we determined backgrounds:

"Information on the offline FIGAERO-CIMS method can be found in previous studies (Siegel et al., 2021; Huang et al., 2019b). However, due to high mass loadings on our filters, we had to adjust the analytical protocol as follows:

1) "sandwich technique" to be able to only use a small punch of the filter. We took 2mm punches of our filter samples and put them between two clean pre-baked (at 200 °C for 1 hour prior to usage) originally sized (25 mm) Zefluor® Teflon filters that fit the FIGAERO filter holder. This allows to reduce the amount of desorbed PM and thus to control reagent ion depletion (shown in Figure S1).

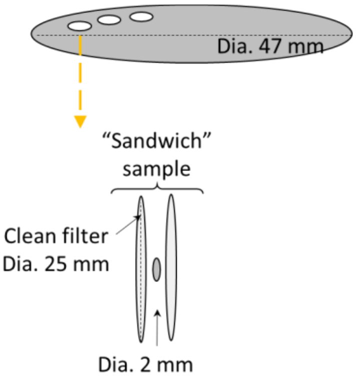

Figure R1 (S1). Schematic of the "sandwich technique" sample preparation

2) "non-uniform temperature ramping" protocol during the FIGAERO-CIMS desorption to reduce the rate of HNO_3 vaporization and thus HNO_3 signal and reagent ion depletion at temperatures between 80 and 100 °C, as following: (1) heating from room temperature (~25 °C) to 60 °C in

8 min, (2) from 60 to 110 °C in 15 min, (3) from 110 °C to 200 °C in 12 min, and (4) held at 200 °C for an additional 20 min (“soak”) (shown in Figure S2).

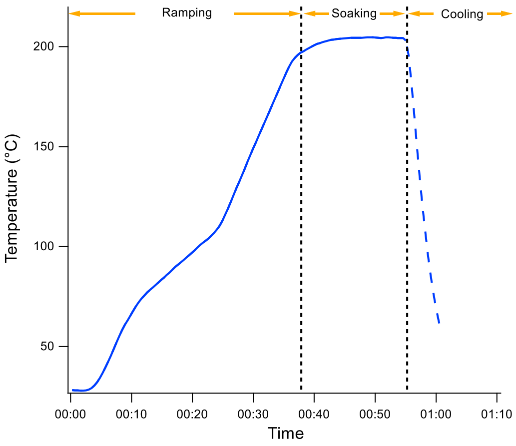

Figure R2 (S2). The FIGAERO-CIMS temperature ramping protocol applied in this study

Background subtraction method to estimate instrumental and field blanks: The variation in instrument background due to the variation in mass loading is taken into account using the signal at maximum heating temperature (200 °C) and thus elevated temperature of surfaces downstream the filter. Thus, the total background signals are the field blanks (average of the 3 blanks) scaled by the signal ratios of ambient sample to blanks of the last 1.5–3 min of the soaking period.”

We assessed the performance of the analytical protocol used by comparing the identified inorganic and total identified organic compounds (CHOX) by offline FIGAERO-CIMS (12-h samples) to the mass concentrations of $PM_{2.5}$ chemical components measured by the co-located ACSM (Figure R3 (new Figure S3)). It shows the time series of the integrated signals of CHOX and inorganic component (HNO_3I^- and SO_3I^-) highly correlated with the OA, NO_3 and SO_4 concentrations from ACSM (Fig. R3, *r*=0.94–0.95).

The main text was also modified and expanded as follows:

“The filters were analyzed using the FIGAERO-CIMS in offline mode, largely following the approach proposed in previous offline FIGAERO-CIMS analyses (Siegel et al., 2021; Huang et al., 2019b). The particles collected on the filter were thermally desorbed by high purity nitrogen gradually heated from room temperature to 200 °C. The desorbed molecules were then charged by the addition of iodide (I^-), which is formed via exposure of methyl iodide to a radioactive source, Po^{210} in this study (Lopez-Hilfiker et al., 2014). The IMR pressure was ~100 mbar and the total ion count (TIC) varied between ~600,000 and 1.2 million counts per second (cps) during analysis. Mass accuracy is within 10 ppm and the mass resolution is between 5000 to 6000 for ions>200 Th. In order to reduce reagent ion depletion, we adapted the analytical protocol as following: 1) we used a “sandwich technique” to hold small punches (2 mm in diameter) of the collected quartz filters (shown in Figure S1), which allowed reduction of the amount of measured $PM_{2.5}$, 2) we used a non-uniform heating protocol for the FIGAERO-CIMS desorption: a slower temperature ramping rate was applied at heating temperatures between 80 and 100 °C to avoid depletion of the reagent ion by the large amount of gaseous HNO_3 evaporating (shown in Figure S2 and S3). More information on the offline method including background determination can be found in the SI.” (Line 102–113)

“The good correlation between FIGAERO-CIMS and ToF-ACSM (CHOX from FIGAERO-CIMS vs OA from ToF-ACSM, HNO_3I^- vs NO_3 from ToF-ACSM, SO_3I^- vs SO_4 from ToF-ACSM, see Figure S3) validates the offline FIGAERO-CIMS analyses – at least in terms of bulk PM constituents – and suggests that artefacts related to the method only play a minor role.” (Line 126–129)

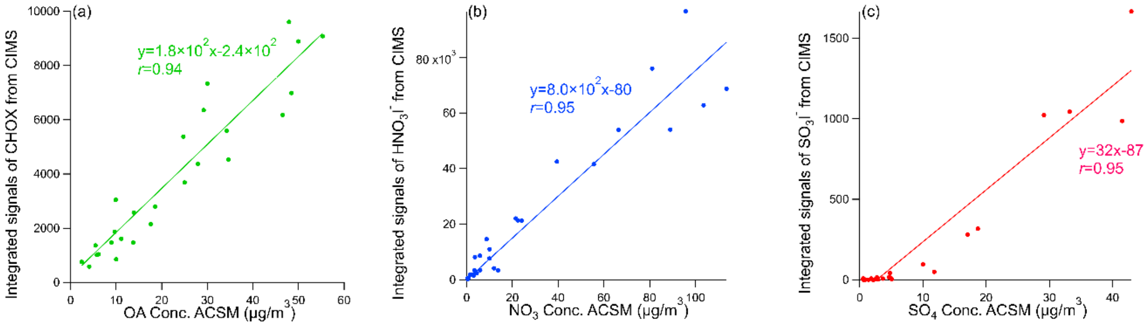

Figure R3 (S3). The comparison between signals from FIGAERO-CIMS and the concentrations of major components of $PM_{2.5}$: (a) CHOX versus OA from ACSM (b) HNO_3I^- versus NO_3 from ACSM, and (c) SO_3I^- versus SO_4 from ACSM

Line 346: Recent paper (Yang et al., 2021) showed that many compounds with high DBE (>2) and oxygen number (>4) are prone to thermal decomposition during FIGAERO heating. Lot of compounds shown in Figure 4 fall into this category, and I would not be surprised that some of the observed compounds could be thermal decomposition products. Authors should consider this possibility and discuss its implications to their results and conclusions.

Reply: We thank the reviewer for pointing out this new publication. We had noticed the recent results on FIGAERO thermal decomposition and double-checked our results accordingly. We would like to point out that the vast majority of signal in our study is from organic compounds with $O_{num}<5$ in both haze and clean periods (Figure R4). A certain degree of thermal decomposition is inevitable for some compounds during the FIGAERO thermal desorption process, mostly for highly functionalized and multifunctional OA compounds (Yang et al., 2021; Stark et al., 2017; Lopez-Hilfiker et al., 2016). However, the high abundance of compounds with DBEs <=2, and O_{num} < 4 such as aldehydes, acids, especially monoacids, and diacids, has been found earlier for Beijing autumn- and wintertime with methods that do not include thermal desorption - such as water-extraction with gas chromatography-FID (GC-FID)/ion chromatography (IC) or organic solvent extraction with gas chromatography-triple quadrupole mass spectrometry (GC/MS/MS) (Guo et al., 2010; Zhao et al., 2018; Yu et al., 2021). It is therefore highly likely that those small compounds are formed by aqueous-phase reactions in winter Beijing as stated in this manuscripts and earlier publications (Lim et al., 2010; Zhao et al., 2018).

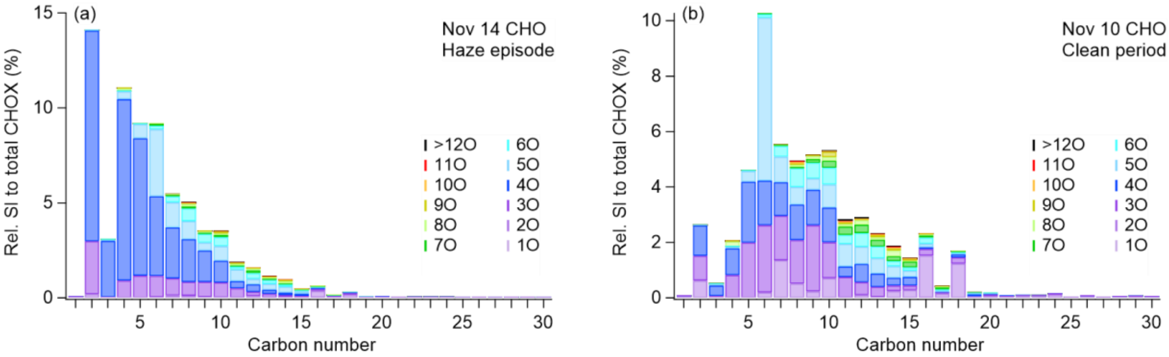

Figure R4 (revised from Figure 3). Signal fractions to total CHOX for CHO compounds with different numbers of oxygen and carbon atoms in (a) Ep3 (Nov 14) periods, (b) the clean period (Nov 10).

We further investigated the possibility of thermal decomposition through the shape of thermograms of these compounds. As thermal fragmentation commonly occurs at temperatures higher than thermal desorption (Buchholz et al., 2020), we expect to see ≥ 2 modes in the thermogram for an ion that is also produced by the thermal decomposition of larger compounds. In Figure R5 (added to the SI as new Figure S18), we present the thermograms of the 10 most abundant OA compounds during the whole sampling period. Note that for thermograms resulting from the non-uniform heating protocol the signal was re-girdded to the temperatures of the uniform temperature ramping protocol. Most of these compounds (7 of 10) show a dominant single-mode in the thermogram and therefore are assumed not to be strongly affected by the thermal decomposition of larger compounds. Two compounds ($C_5H_6O_4I^-$ and $C_6H_8O_4I^-$) showed two modes in their thermograms with higher signals for the first mode. Only one compound ($C_2H_4O_3I^-$) seemed to be mostly a thermal fragment, as its signal is strongly dominated by the second mode at the higher temperature. Based on similar checks (Figure R7), we estimated that for the key compounds for light absorption (Figure 6), most of the small compounds (C_{num}<6) in the CHO (72%, 5/7), and CHON or CHOS (73%, 8/11) groups are not significantly influenced by thermal desorption. For five compounds ($C_4H_6O_5I^-$, $C_5H_{12}O_5I^-$, $C_5H_3NO_3I^-$, $C_4H_5NO_3I^-$, $C_6H_5NO_4I^-$), however, the signal can be influenced by thermal desorption due to their relatively strong second thermogram peaks. We have also slightly revised Figure 6 (Figure R6) in the manuscript and marked those species by * in the axis labels.

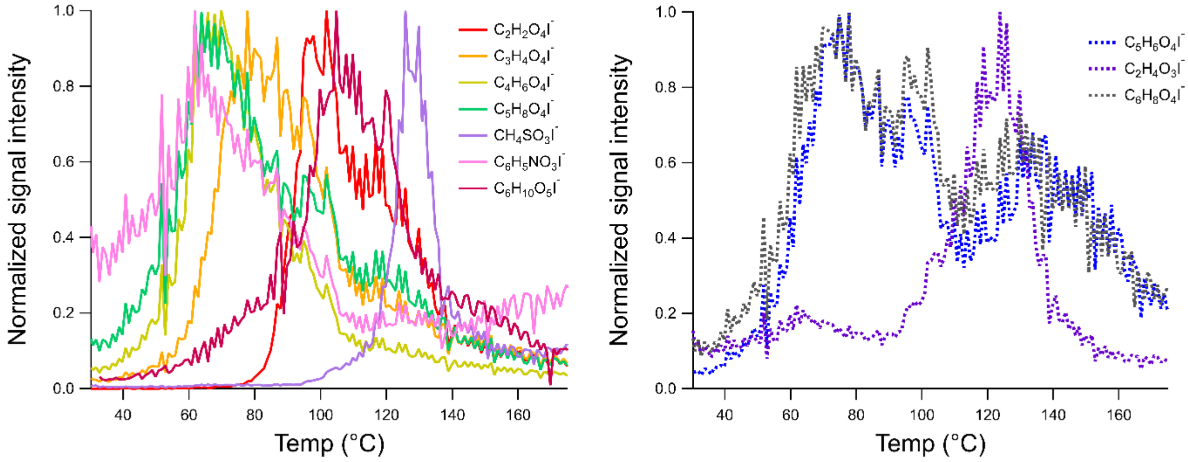

Figure R5 (Figure S18). Normalized thermograms of the ions of (a) $C_2H_2O_4I^-$, $C_3H_4O_4I^-$, $C_4H_6O_4I^-$, $C_5H_8O_4I^-$, $CH_4SO_3I^-$, $C_6H_5NO_3I^-$, $C_7H_7NO_3I^-$ and (b) $C_5H_6O_4I^-$, $C_2H_4O_3I^-$, $C_6H_8O_4I^-$, on Nov 14. The thermograms were normalized by the maximum signals during the desorption.

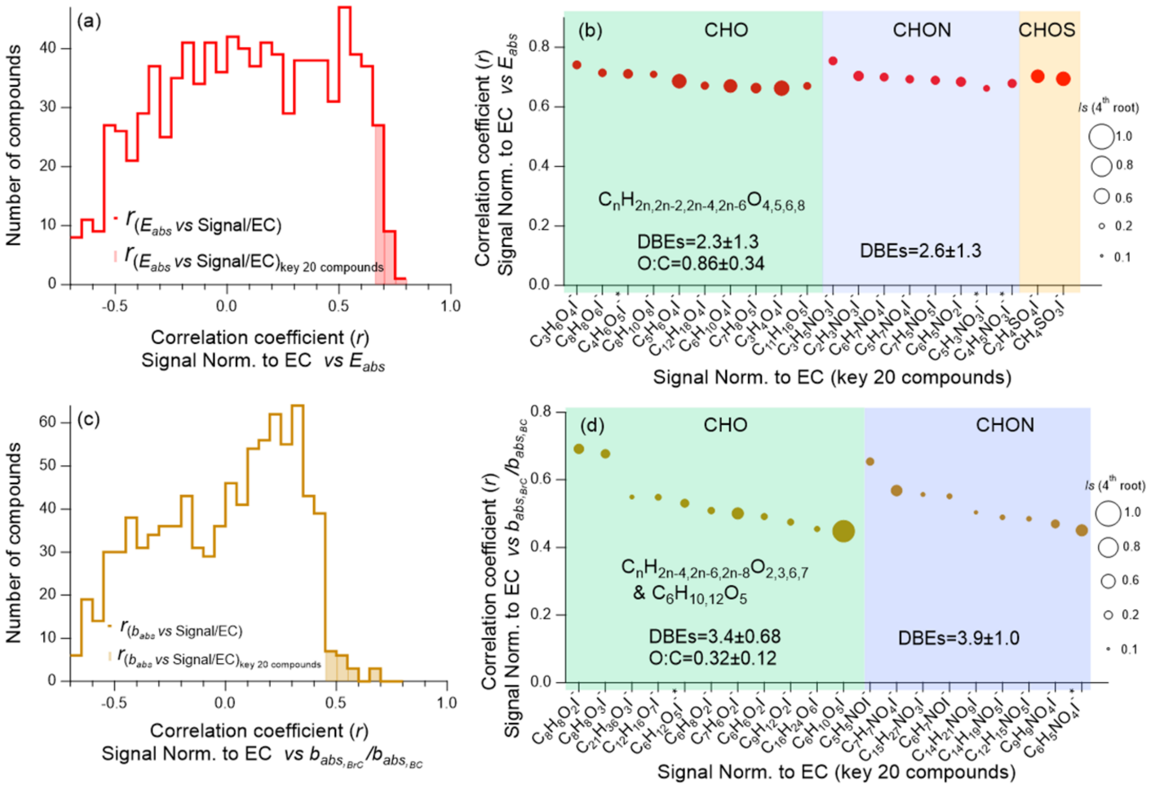

Figure R6 (Figure 6). (a) Histogram of the correlation coefficients (*r*) between the normalized OA signals and E_{abs} at 880 nm for all identified compounds (red line) and the key 20 compounds (red shaded area), (b) the correlation coefficients of key 20 compounds for E_{abs} at 880 nm, (c) histogram of the correlation coefficients between the normalized OA compound signals and $b_{abs,\ BrC}/b_{abs,\ BC}$ at 370nm for all identified compounds (brown line) and the key 20 compounds (brown shaded area), and (d) the correlation coefficients of key 20 compounds for $b_{abs,BrC}/b_{abs,BC}$ at 370nm. The size of the symbols in (b) and (d) is proportional to the 4th root of the average signal intensities of the corresponding compound during the whole sampling period. Compounds that possibly have a substantial contribution of larger thermally fragmented parent compounds are marked with * in the axis labels..

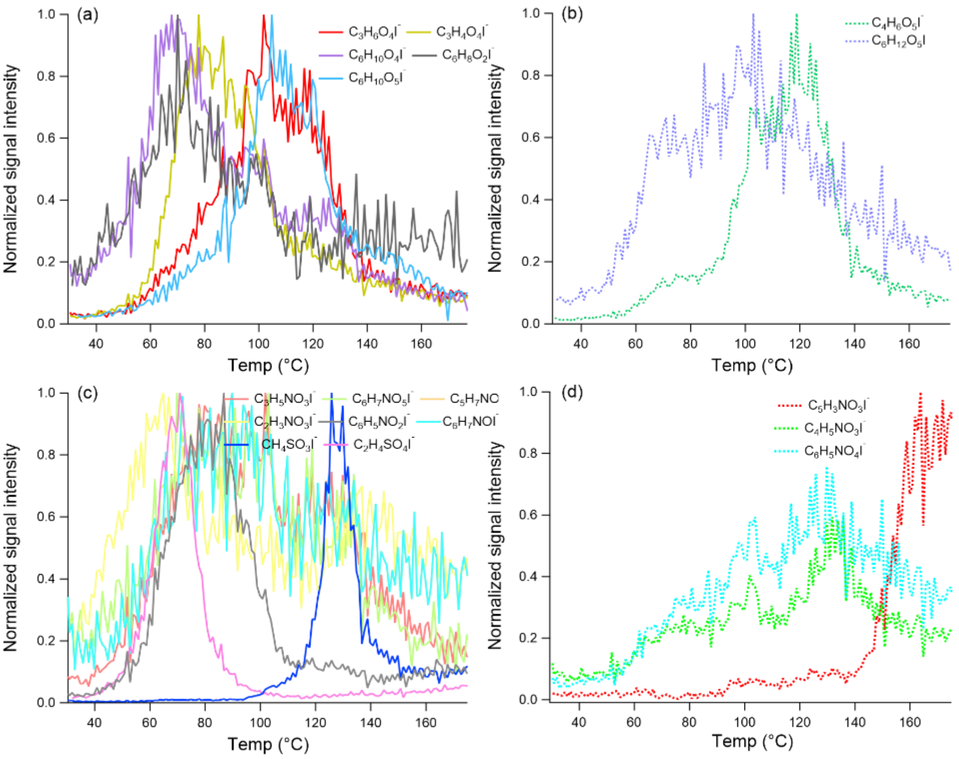

Figure R7 (Figure S19). Normalized thermograms of the ions of the 18 key compounds on Nov 14 with $C_{num}≤6$ in Figure 6 (a) CHO group compounds without strong influence by thermal decompositions, and (b) CHO group compounds with a potentially strong influence by thermal decompositions, (c) CHON group compounds without strong influence by thermal decompositions and (d) CHON group compounds a potentially strong influence by thermal decompositions. The thermograms were normalized by the maximum signals during the desorption.

The main text in the revised manuscript was modified as follows:

Main text

"Chemical characterization by FIGAERO-CIMS, essentially a thermodesorption technique, is prone to thermal decomposition. For example, more oxygenated multi-functional organic compounds such as citric acid ($C_6H_8O_7$) and sucrose ($C_{12}H_{22}O_{11}$) were found to be affected by thermal decomposition in the FIGAERO-CIMS (Yang et al., 2021; Stark et al., 2017). Since thermal decomposition generally occurs at temperatures higher than the desorption temperature of most compounds (Buchholz et al., 2020), multi-modal thermogram shapes can be used as an indicator for signal contributions from thermally fragmented compounds. Based on such analysis of the filter collected on Nov 14, among the 10 ions with the highest intensity, only one ($C_2H_4O_3I^-$) appeared to be affected strongly by thermal decomposition (Figure S18)." (Line 136–142)

"Among those key species, in Figure 6 we marked the compounds that, according to their thermograms, likely are influenced by thermal decomposition ($C_4H_6O_5I^-$, $C_5H_{12}O_5I^-$, $C_5H_3NO_3I^-$, $C_4H_5NO_3I^-$, $C_6H_5NO_4I^-$). Most of the other small compounds ($C_{num}<6$) in the CHO (72%, 5/7), and CHON or CHOS (73%, 8/11) groups are not significantly influenced by thermal desorption." (Line 450–453)

Minor comments:

Section 2: The information about the used CIMS should be more detailed, for example the model, mass resolving power, ect should be presented. Also details of the used I- nitrogen flow and IMR pressure are missing.

Reply: more information on CIMS settings has been added in the revised manuscript (compare also the response to the first main comment)

Main text

"The filters were analyzed using the FIGAERO-CIMS in offline mode, largely following the approach proposed in previous offline FIGAERO-CIMS analyses. The particles collected on the filter were thermally desorbed by high purity nitrogen gradually heated from room temperature to 200 °C. The desorbed molecules were then charged by the addition of iodide (I^-), which is formed via exposure of methyl iodide to a radioactive source, Po^{210} in this study (Lopez-Hilfiker et al., 2014). The IMR pressure was ~100 mbar and the total ion count (TIC) varied between ~600,000 and 1.2 million counts per second (cps) during analysis. Mass accuracy is within 10 ppm and the mass resolution is between 5000 to 6000 for ions>200 Th. In order to reduce reagent ion depletion, we adapted the analytical protocol as following: 1) we used a "sandwich technique" to hold small punches (2 mm in diameter) of the collected quartz filters (shown in Figure S1), which allowed reduction the amount of measured $PM_{2.5}$, 2) we used a non-uniform heating protocol for the FIGAERO-CIMS desorption: a slower temperature ramping rate was applied at heating temperatures between 80 and 100 °C to avoid depletion of the reagent ion by the large amount of gaseous HNO_3 evaporating (shown in Figure S2 and S3). More information on the offline method including background determination can be found in the SI." (Line 102–113)

Line 95: Some estimation of collected particulate mass on the filters should be presented.

Reply: the loadings of $PM_{2.5}$ and OA mass on the filters calculated from ToF-ACSM measurements have been added in the revised Table S1 as suggested

Table S1 Sampling information and mass loadings on the punches

Sampling date	Sampling time	NR-PM$_{2.5}$+BC loading (µg/punch)	OA loading (µg/punch)
Nov 3	9:30–21:00	3.87	1.04
	21:30–9:00	4.11	1.00
Nov 4	9:30–21:00	0.63	0.23
	21:30–9:00	0.28	0.13
Nov 5	9:30–21:00	0.61	0.20
	21:30–9:00	0.48	0.21
Nov 6	9:30–21:00	NaN	NaN
	21:30–9:00	0.57	0.37
Nov 7	9:30–21:00	0.58	0.25
	21:30–9:00	1.02	0.52
Nov 8	9:30–21:00	1.51	0.61
	21:30–9:00	1.49	0.62
Nov 9	9:30–21:00	0.17	0.12
	21:30–9:00	0.14	0.09
Nov 10	9:30–21:00	0.33	0.21
	21:30–9:00	0.49	0.29
Nov 11	9:30–21:00	0.77	0.29
	21:30–9:00	1.30	0.52
Nov 12	9:30–21:00	2.03	0.58
	21:30–9:00	2.70	0.72
Nov 13	9:30–21:00	4.84	1.01
	21:30–9:00	5.57	1.15
Nov 14	9:30–21:00	4.65	0.97
	21:30–9:00	3.43	0.71
Nov 15	9:30–21:00	0.22	0.11
	21:30–9:00	0.09	0.05
Nov 16	9:30–21:00	0.32	0.19
	21:30–9:00	0.65	0.39
Oct 26, Nov 4, Nov 17 (blanks)			

Note: Field blanks were collected by putting in the sample holder for 10 minutes without activating the sampling flow and were later analyzed using the same method as the samples

Line 96: Sampling dates for the three blanks are missing from the Figure 1 and Table S1.

Reply: the field blanks were collected before (Oct 26), during (Nov 4), and after (Nov 17) the sampling period.

The sampling dates for the three blanks are now listed in the revised Table S1

Line 97: How long was the time between measurement and off-line analysis? Chemical reactions are possible overtime, even if the filters have been stored in freezer. Was the FIGAERO-CIMS analysis done in the same location as the measurements?

Reply: After collection, the filters were kept in the filter holders, wrapped in aluminum foil, sealed in bags, and kept in a freezer at -20 °C until analysis at Stockholm University 7 months later. The filters were transported in a thermally insulated box with ice packs. The good agreement in relative signal between our offline method and the online measurements by the ToF-ACSM indicate our results to be sound. We added the following information in the main text.

“Samples were kept in the filter holders, wrapped in aluminum foil, sealed in bags, and kept in a freezer at -20 °C until analysis at Stockholm University 7 months after collection. The filters were transported in a thermally insulated box with ice packs.” (Line 98–100)

“The good correlation between FIGAERO-CIMS and ToF-ACSM (CHOX from FIGAERO-CIMS vs OA from ToF-ACSM, HNO_3I^- vs NO_3 from ToF-ACSM, SO_3I^- vs SO_4 from ToF-ACSM, see Figure S3) validates the offline FIGAERO-CIMS analyses – at least in terms of bulk PM constituents – and suggests that artefacts related to the method only play a minor role.” (Line 126–129)

Line 101: Elaborate what does “pre-baked” mean.

Reply: Pre-baked means these filters were baked at 200 °C for 1 hour prior to usage. This information was added to the SI:

“…and put them between two pre-baked (baked at 200 °C for 1 hour prior to usage) originally sized (25 mm) Zefluor® Teflon filters that fit the FIGAERO filter holder (“sandwich technique”)…”

Line 198: Episode periods could be marked more visibly in the Figure 1 plots, now its a bit guessing about the correct time periods.

Reply: now Figure 1 and its caption have been revised as follows to better present the periods:

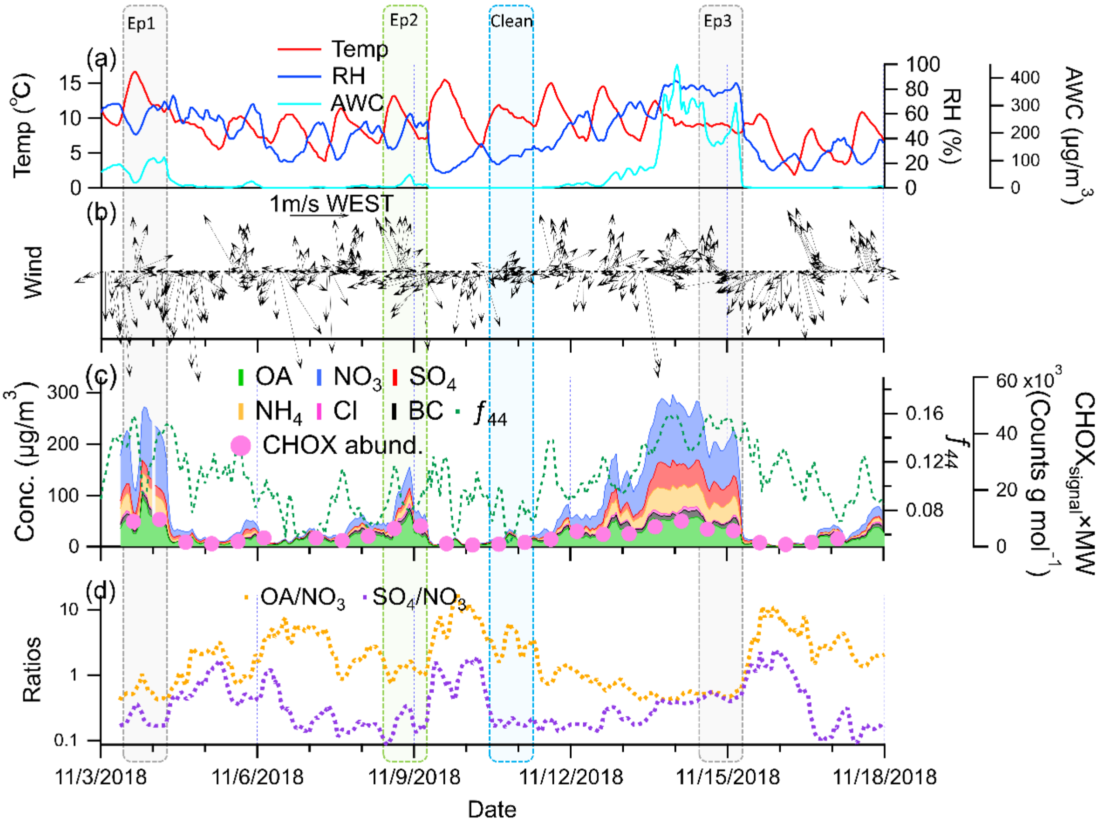

Figure R8 (Figure 1). Time series of (a) temperature, relative humidity (RH), aerosol water content (AWC), (b) 1-hour averaged wind direction and wind speed, (c) chemical components of NR-$PM_{2.5}$, BC, ƒ44 from ACSM, CHOX abundance from FIGAERO-CIMS and their sampling dates are marked by pink dots, (d) OA/NO_3 and SO_4/NO_3. The sampling time of episode days is marked by boxes, which last from 9:30 am to 9:00 am the next day.

Line 363: Indicate which panel of the Figure S4 is in question.

Reply: now the sentence has been revised to:

"an influence of southern areas at the receptor site, where residential biomass burning emissions are abundant (Figure S8 (c) and (g))." (Line 391–392)

Line 364-366: This comparison could be more illustrative in a Table. Now it's somewhat hard to follow.

Reply: Thanks for the suggestion. Now the comparison for different episodes has been summarized in Table S2 and is referred to in the main text.

Table S2 Comparison of absolute integrated signal (*Is*) of some major compounds for different episodes

	Absolute *Is* (count)			
ions	Ep1	Ep2	Ep3	Clean
HNO_3I^-	1381	337	854	30
SO_3I^-	3.96	0.10	13.32	0.02
$CH_4SO_3I^-$	1.00	0.48	0.79	0.01
$C_2H_4SO_4I^-$	0.92	0.11	0.86	0.00
$C_2H_2O_4I^-$	3.45	0.58	3.85	0.05
$C_3H_4O_4I^-$	1.22	0.29	0.97	0.01
$C_4H_6O_4I^-$	1.25	0.41	2.35	0.03
$C_5H_8O_4I^-$	1.57	1.99	1.62	0.12
$C_6H_{10}O_5I^-$	1.86	8.51	0.91	0.51
$C_6H_5NO_4I^-$	0.22	0.60	0.08	0.03
$C_7H_7NO_4I^-$	0.12	0.33	0.05	0.05

Line 369: Indicate which panel is in question in Figure 4.

Reply: it has been revised as follows:

"As shown in Figure 4 (c), (e) and (g), a homologous-like series of dicarboxylic acids ($C_nH_{2n-2}O_4$) and a series of compounds with one or more DBEs ($C_nH_{2n-4}O_4$) were enhanced in Ep1 and Ep3 compared to Ep2." (Line 398–400)

Line 398: Is there reference to a wrong figure here?

Reply: now it has been corrected to:

"indicating that BC particles were more aged and more thickly coated by organic and inorganic constituents (Figure S17)." (Line 433)

Line 401: Is the data shown in Figure S12 from the whole campaign? If so, it should be clarified in the caption so that reader does not think that different panels represent different episodes

Reply: Thanks for the suggestion. Now the figure caption of Figure S16 has been revised to:

"E_{abs} at different wavelengths as a function of (a) POA/EC, (b) SOA/EC and (c) SIA/EC during the whole sampling period"

Line 401: Acronym "POA" is not defined in the text.

Reply: Line 401 has been revised as follows:

“Here, we show E_{abs} variation as a function of SIA, primary organic aerosol (POA), and SOA to EC ratios (Figure S16).” (Line 436)

Reference

Buchholz, A., Ylisirniö, A., Huang, W., Mohr, C., Canagaratna, M., Worsnop, D. R., Schobesberger, S., and Virtanen, A.: Deconvolution of FIGAERO–CIMS thermal desorption profiles using positive matrix factorisation to identify chemical and physical processes during particle evaporation, Atmospheric Chemistry and Physics, 20, 7693-7716, 10.5194/acp-20-7693-2020, 2020.

Guo, S., Hu, M., Wang, Z. B., Slanina, J., and Zhao, Y. L.: Size-resolved aerosol water-soluble ionic compositions in the summer of Beijing: implication of regional secondary formation, Atmos. Chem. Phys., 10, 947-959, 10.5194/acp-10-947-2010, 2010.

Huang, W., Saathoff, H., Shen, X., Ramisetty, R., Leisner, T., and Mohr, C.: Seasonal characteristics of organic aerosol chemical composition and volatility in Stuttgart, Germany, Atmospheric Chemistry and Physics Discussions, 1-22, 10.5194/acp-2019-364, 2019a.

Huang, W., Saathoff, H., Shen, X., Ramisetty, R., Leisner, T., and Mohr, C.: Seasonal characteristics of organic aerosol chemical composition and volatility in Stuttgart, Germany, Atmospheric Chemistry and Physics, 19, 11687-11700, 10.5194/acp-19-11687-2019, 2019b.

Lim, Y. B., Tan, Y., Perri, M. J., Seitzinger, S. P., and Turpin, B. J.: Aqueous chemistry and its role in secondary organic aerosol (SOA) formation, Atmospheric Chemistry and Physics, 10, 10521-10539, 10.5194/acp-10-10521-2010, 2010.

Lopez-Hilfiker, F. D., Iyer, S., Mohr, C., Lee, B. H., D'Ambro, E. L., Kurtén, T., and Thornton, J. A.: Constraining the sensitivity of iodide adduct chemical ionization mass spectrometry to multifunctional organic molecules using the collision limit and thermodynamic stability of iodide ion adducts, Atmospheric Measurement Techniques, 9, 1505-1512, 10.5194/amt-9-1505-2016, 2016.

Lopez-Hilfiker, F. D., Mohr, C., Ehn, M., Rubach, F., Kleist, E., Wildt, J., Mentel, T. F., Lutz, A., Hallquist, M., Worsnop, D., and Thornton, J. A.: A novel method for online analysis of gas and particle composition: description and evaluation of a Filter Inlet for Gases and AEROsols (FIGAERO), Atmospheric Measurement Techniques, 7, 983-1001, 10.5194/amt-7-983-2014, 2014.

Siegel, K., Karlsson, L., Zieger, P., Baccarini, A., Schmale, J., Lawler, M., Salter, M., Leck, C., Ekman, A. M. L., Riipinen, I., and Mohr, C.: Insights into the molecular composition of semi-volatile aerosols in the summertime central Arctic Ocean using FIGAERO-CIMS, Environmental Science: Atmospheres, 10.1039/d0ea00023j, 2021.

Stark, H., Yatavelli, R. L. N., Thompson, S. L., Kang, H., Krechmer, J. E., Kimmel, J. R., Palm, B. B., Hu, W., Hayes, P. L., Day, D. A., Campuzano-Jost, P., Canagaratna, M. R., Jayne, J. T., Worsnop, D. R., and Jimenez, J. L.: Impact of Thermal Decomposition on Thermal Desorption Instruments: Advantage of Thermogram Analysis for Quantifying Volatility Distributions of Organic Species, Environ Sci Technol, 51, 8491-8500, 10.1021/acs.est.7b00160, 2017.

Yang, L. H., Takeuchi, M., Chen, Y., and Ng, N. L.: Characterization of thermal decomposition of oxygenated organic compounds in FIGAERO-CIMS, Aerosol Science and Technology, 1-22, 10.1080/02786826.2021.1945529, 2021.

Yu, Q., Chen, J., Cheng, S., Qin, W., Zhang, Y., Sun, Y., and Ahmad, M.: Seasonal variation of dicarboxylic acids in PM2.5 in Beijing: Implications for the formation and aging processes of secondary organic aerosols, Sci Total Environ, 763, 142964, 10.1016/j.scitotenv.2020.142964, 2021.

Zhao, W., Kawamura, K., Yue, S., Wei, L., Ren, H., Yan, Y., Kang, M., Li, L., Ren, L., Lai, S., Li, J., Sun, Y., Wang, Z., and Fu, P.: Molecular distribution and compound-specific stable carbon isotopic composition of dicarboxylic acids, oxocarboxylic acids and <i>α</i>-dicarbonyls in PM<sub>2.5</sub> from Beijing, China, Atmospheric Chemistry and Physics, 18, 2749-2767, 10.5194/acp-18-2749-2018, 2018.